

Oxygen ordering and phase separation in $\text{La}_2\text{CuO}_{4+\delta}$

B. W. Statt,* P. C. Hammel, and Z. Fisk
Los Alamos National Laboratory, Los Alamos, New Mexico 87545

S-W. Cheong
AT&T Bell Laboratories, Murray Hill, New Jersey 07974

F. C. Chou and D. C. Johnston
Ames Laboratory, Iowa State University, Ames, Iowa 50011

J. E. Schirber
Sandia National Laboratories, Albuquerque, New Mexico 87185
(Received 10 July 1995)

We present a detailed NMR study of the expected *A* and anomalous *B* Cu lines on a single crystal of $\text{La}_2\text{CuO}_{4+\delta}$. Our results in conjunction with those of neutron scattering and La NMR lead us to conclude that oxygen ordering occurs on a microscopic scale in this compound. The ordered interstitial oxygen gives rise to a distribution of tilts of the CuO_6 octahedra in the *B* domains. A sawtooth modulation of the octahedral tilt, in which the sign of the tilt changes when the tilt reaches a maximum value, is deduced. In addition we show that macroscopic phase separation is inhibited in the tetragonal phase where the CuO_6 octahedra are not tilted.

I. INTRODUCTION

Considerable progress has been made in understanding the electronic and magnetic properties of the cuprate superconductors. Much of this implicitly assumes a homogeneous underlying crystal structure and electronic density. It is becoming increasingly apparent that there exist variations in these properties on length scales varying from the lattice constant to macroscopic scales in various cuprates. Here we will discuss aspects of two such inhomogeneities in oxygen doped $\text{La}_2\text{CuO}_{4+\delta}$. The first is the suppression of macroscopic phase separation in the tetragonal phase. Next we will discuss the interplay between ordering of the interstitial oxygen dopants and the tilt angle of the CuO_6 octahedra. This leads to a microscopic ordering of the interstitial oxygens.

There is considerable evidence that the tendency toward phase separation is a universal feature of doped cuprates.^{1,2} However macroscopic phase separation is prevented in general by the large Coulomb energy cost of concentrating doped holes into droplets. In $\text{La}_2\text{CuO}_{4+\delta}$ macroscopic phase separation is made possible by the mobility of the interstitial oxygen dopants which follow the holes and maintain charge neutrality in the hole rich regions and eliminate the Coulomb energy cost. However some details of macroscopic phase separation in $\text{La}_2\text{CuO}_{4+\delta}$ remain unclear. Based on the coincidence between the macroscopic phase separation temperature T_{PS} and the temperature T_{TO} of the tetragonal to orthorhombic phase transition at two points widely separated in temperature, we propose that the macroscopic phase separation is inhibited in the tetragonal phase and occurs at the structural phase transition temperature because the tilting of the CuO_6 octahedra allows enhanced oxygen mobility within the La-O layers.

In the second portion of this work we will discuss an inhomogeneity in the CuO_2 planes on the scale of several

lattice constants for the oxygen-rich metallic phase. Neutron scattering studies³ indicate that the interstitial oxygen dopants in $\text{La}_2\text{CuO}_{4+\delta}$ may be ordered. ^{139}La NMR studies⁴ have demonstrated that instead of a single, well-defined tilt of the CuO_6 octahedra there is in fact a uniform distribution of tilts. We propose that this distribution is the consequence of a one-dimensional modulation of the octahedral tilts in which the tilt increases linearly with position in a direction parallel to the diagonal of the orthorhombic unit cell of the crystal: a *tilt wave*. If, when the tilt exceeds a certain cutoff angle it abruptly shifts to a rotation of the same magnitude but opposite sense, this will leave a large opening in the La-O layer which will more easily accommodate the interstitial oxygen. This mechanism naturally leads to ordering of interstitial oxygen into stripes.

Crystallographically there is a single unique copper site in lanthanum cuprate. However, two distinct spectral lines are observed in the Cu NQR spectrum of the doped material^{5,6} which unequivocally demonstrate the existence of two copper sites. The NQR frequency of the two lines is independent of the method of doping (Sr or O doping) demonstrating that the second copper site is not distinguished by the presence of the dopant itself, but is the result of the presence of doped holes. We have determined that the second copper site is adjacent to the stripe ordered interstitial oxygens thus indicating that the anomalous copper sites form striped domains. The combination of the ^{139}La NMR and ^{63}Cu NMR results make a compelling argument for the *tilt wave* and oxygen ordering in $\text{La}_2\text{CuO}_{4+\delta}$. Finally, we present evidence that the NQR frequency of the anomalous copper site indicates that it neighbors a CuO_4 plaquette occupied by a static or pinned hole. The propensity of holes toward pinning in the CuO_2 planes is surprising and this should be taken into account in considering electronic and magnetic behavior in the cuprates.

II. PHASE SEPARATION AND THE T-O TRANSITION

There is good evidence that fluctuating, microscopic phase separation is a ubiquitous phenomenon in cuprate superconductors.^{1,2} The observation of static and macroscopic phase separation in oxygen doped $\text{La}_2\text{CuO}_{4+\delta}$ provides an opportunity to study at least some aspects of this phenomenon. It is important, however, to understand the relationship between the electronic phase separation which is thought to be the driving force behind this phenomenon and the mobility of the oxygen ions which enables the phase separation to exist on a macroscopic scale by eliminating the Coulomb energy which develops when charge holes phase separate in a rigid ionic background. Neutron diffraction measurements⁷ have provided information about both the phase separation temperature and the tetragonal to orthorhombic (TO) structural phase transition in $\text{La}_2\text{CuO}_{4+\delta}$. They observe that phase separation coincides with the TO transition at $(T, \delta) = (430 \text{ K}, 0.035)$, and $(380 \text{ K}, 0.039)$. Our NMR measurements demonstrate a similar coincidence at $T \approx 260 \text{ K}$. This implies a coincidence of the phase separation and structural phase transition lines in the phase diagram. We will argue here that the TO phase transition enables the macroscopic phase separation and this is probably due to the fact that oxygen mobility is improved in the orthorhombic phase. This implies that in the tetragonal region of the phase diagram, roughly defined by $0.03 < \delta < 0.05$ and $260 \text{ K} < T < 415 \text{ K}$, there is a tendency toward phase separation, but that macroscopic phase separation is suppressed by lack of oxygen mobility. We are unable to make any statements concerning whether the driving force behind phase separation is electronic or driven by a chemical phase separation of the excess oxygen. However, this view is in agreement with and thus supports the earlier described picture² that there exist cuprates having the tendency toward phase separation but for which macroscopic phase separation is prevented by lack of counter-ion mobility. It also provides some insight into the peculiar shape of the phase separation diagram in oxygen doped $\text{La}_2\text{CuO}_{4+\delta}$.

¹³⁹La NMR is an excellent probe of the local octahedral tilt in those samples having a sharp ¹³⁹La NMR line.⁶ Furthermore, Büchner *et al.* have persuasively argued⁸ that the magnitude of this tilt is directly correlated with the magnitude of the orthorhombic order parameter. Thus we are able to use NMR to accurately determine the TO phase transition temperature.¹³⁹La NMR is also sensitive to the onset of macroscopic phase separation.⁹ We have found a distribution of octahedral tilts in the orthorhombic metallic phase, probably arising from a long wavelength *tilt wave* (we will discuss this further below). Nonetheless, there is a well-defined temperature above which the material is tetragonal (i.e., there is no tilt). Figure 1 shows the temperature dependence of the average tilt of the octahedra. Within the experimental error, this vanishes at the macroscopic phase separation temperature of 260 K. In Fig. 2 we show our data for the temperature and oxygen content of the two phases of a sample prepared with an overall oxygen content of 4.04.¹⁰ Radaelli *et al.* have recently published data⁷ for the macroscopic phase separation temperature and the TO phase transition temperature for samples prepared with several different oxygen contents. Some of these data are also shown in Fig. 2. They find a

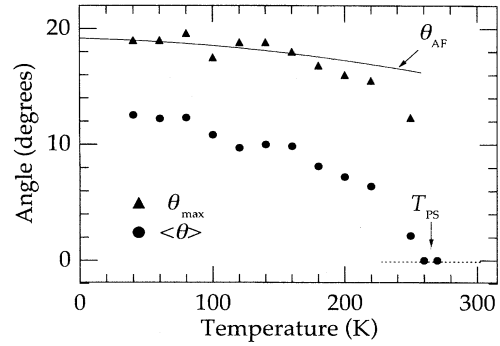


FIG. 1. The temperature dependencies of two parameters describing the tilt of V_z are shown. These two parameters are $\langle \theta \rangle = \cos^{-1} \langle \mu \rangle$ where the distribution of μ is given by $P(\mu)$ and $\langle \mu \rangle = \int \mu P(\mu) d\mu / \int P(\mu) d\mu$. There are no tilts greater than the cutoff angle θ_{\max} . The tilt vanishes in the tetragonal phase, thus the tetragonal to orthorhombic (TO) phase transition is indicated by the onset of tilting. The macroscopic phase separation coincides with the TO phase transition temperature.

sample having an oxygen content $\delta = 0.032$ for which the macroscopic phase separation and the TO phase transition occur simultaneously at a temperature of 415 K. They also infer that these two temperatures coincide at $\delta = 0.039$ and 380 K.

This suggests that the phase separation and structural phase transition lines coincide between 415 K and 260 K indicating a strong interrelationship between the two transitions. The TO structural phase transition temperature is decreasing very rapidly with increasing oxygen content in this region. The coincidental strong decrease of the macroscopic phase separation temperature further suggests that phase

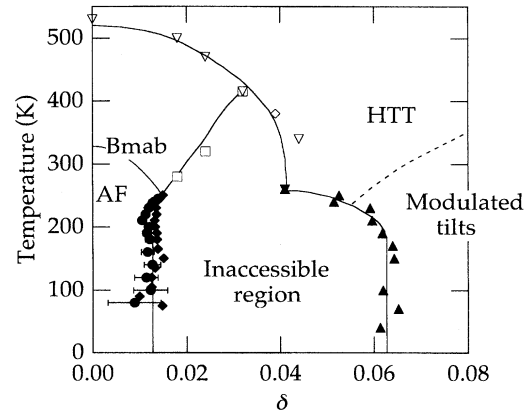


FIG. 2. Phase diagram for oxygen doped $\text{La}_2\text{CuO}_{4+\delta}$. Shown in this diagram are data for both the macroscopic phase separation temperature (squares, circles, diamonds, and triangles) and the TO phase transition temperature (inverted triangles and diamond). Open symbols are from Radaelli *et al.* Phase separation coincides with the structural phase transition between two widely separated temperatures: 415 K and 260 K. The point (open diamond) at 380 K and $\delta = 0.039$ is the point at which the oxygen rich phase undergoes the TO phase transition.

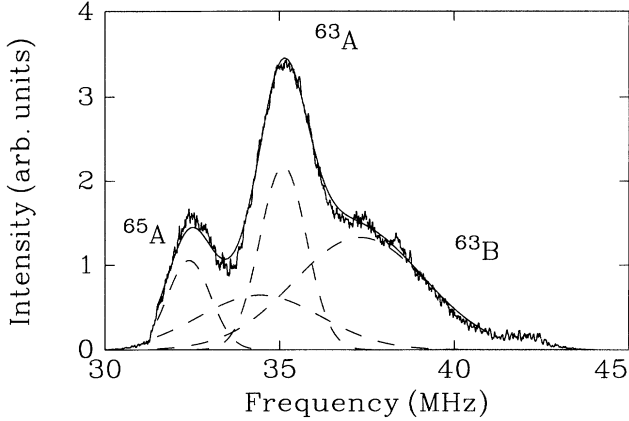


FIG. 3. NQR spectrum of $\text{La}_2\text{CuO}_{4.1}$ taken at $T=79$ K. Note that the *A* and *B* lines are in duplicate, one from each copper isotope, ^{63}Cu and ^{65}Cu .

separation is suppressed in the tetragonal phase. High oxygen mobilities are required for macroscopic phase separation, and this result indicates that only the orthorhombic phase allows this. The interstitial oxygen resides between the La_2O_2 layers.^{3,11} The orthorhombic phase is characterized by a tilting of the octahedra.⁸ This involves lateral motions of the apical oxygens which produce larger openings in the La_2O_2 layer. It is plausible that this enhances lateral oxygen mobilities through the La_2O_2 layers which may in turn enable macroscopic phase separation.

The observation that the macroscopic phase separation line coincides with the TO structural phase transition line indicates a direct coupling between the crystal structure of $\text{La}_2\text{CuO}_{4+\delta}$ and the accessibility of macroscopic phase separation. This recognition adds to our understanding of the rather unusual shape of the phase separation phase curve in this material. [We note, however, that one point at oxygen content ($\delta \approx 0.044$) reported by Radaelli *et al.* does not fit easily into this simple picture.] This observation is also significant in that it indicates that for certain values of the doping and temperature in the tetragonal phase, there is a tendency toward phase separation which is unable to manifest itself on a macroscopic scale. Thus, $\text{La}_2\text{CuO}_{4+\delta}$ in addition to displaying macroscopic phase separation in the orthorhombic phase, may provide an example of phase separation which is frustrated by lack of counter-ion mobility in the tetragonal phase. This would then be an example of the phenomenon of frustration of macroscopic phase separation² which is thought to prevail in the majority of the cuprates which do not have highly mobile ions at the low temperatures at which phase separation would have occurred.

III. Cu NMR EXPERIMENT: OXYGEN ORDERING

Crystallographic studies of doped lanthanum cuprate, which reveal the average crystal structure, find a single copper site *A*. On the other hand, microscopic probes of local structure such as nuclear quadrupole resonance (NQR) find that lanthanum cuprate, whether doped by cation substitution (e.g., Sr doped) or by excess oxygen has two distinct spectral lines.^{5,6} A Cu NQR spectrum is shown in Fig. 3. This is

unequivocal evidence for a second, anomalous copper site *B*. The disturbance of the lattice associated with the presence of these two types of dopant are very different in the case of substitutional Sr and interstitial oxygen. The facts that the Cu NQR frequencies are independent of the means of doping and that undoped La_2CuO_4 exhibits a single line,¹² indicate that the anomalous site is not the consequence of this disturbance, rather it must be associated with the presence of doped holes. NQR reveals structure averaged over time scales of approximately a microsecond so this structural feature must be essentially static. The intensity of the two spectral lines shows that there are significant numbers of anomalous copper sites, particularly in the O doped material. We now discuss in detail our analysis of the Cu NMR results.

The single crystal of $\text{La}_2\text{CuO}_{4.1}$ used in this work was grown first as La_2CuO_4 by a flux method. Electrochemical oxidation was then used to dope the crystal.¹³ dc magnetization measurements show a superconducting onset temperature of about 40 K. Standard pulse techniques were used to obtain the field dependent NMR line shapes at 50 K.

The copper NQR line shape is inhomogeneously broadened by the distribution of EFG's throughout the crystal. In the NQR case ($H_0 = 0$) small tilts in the EFG principle axis have little effect on the line shape. Only the magnitude of the EFG is relevant in determining the local NQR frequency ν_Q . On the other hand the NMR line shape ($H_0 \neq 0$) is broadened not only by the distribution in EFG magnitudes but also by the distribution in EFG tilts. As copper nuclei have spin 3/2 there is a central transition ($1/2 \leftrightarrow -1/2$) and two satellite transitions ($\pm 3/2 \leftrightarrow \pm 1/2$). To second order in the quadrupolar frequency ν_Q the central transition resonance frequency is given by

$$\nu_0 = \nu_L + \frac{\nu_Q^2}{\nu_L} \left(h(\theta) - \frac{\eta}{8} \sin^2 \theta (1 + 9 \cos^2 \theta) \cos 2\phi \right), \quad (1)$$

where ν_L is the Larmor frequency, η is the EFG asymmetry parameter, and θ and ϕ are the angles of the EFG principle axes with respect to H_0 . The function $h(\theta) = -3/8 \sin^2 \theta + 3/16 \sin^4 \theta$. To first order in ν_Q the satellite resonance frequency is given by

$$\nu_0 = \nu_L \pm \nu_Q (3/2 \cos^2 \theta - 1/2 - 1/2 \eta \sin^2 \theta \cos 2\phi). \quad (2)$$

For large H_0 the distribution of ν_Q will broaden the central transition linewidth less than the satellites. Thus we focus on the central line shape with its larger peak intensity.

We obtain ν_Q from the NQR spectrum displayed in Fig. 3. Fitting this spectrum to Gaussians with the appropriately constrained ^{63}Cu , ^{65}Cu isotopic parameters we find $\nu_Q^A = 35.1$ MHz and $\nu_Q^B = 37.3$ MHz for ^{63}Cu . The full width at half maximum (FWHM) are found to be $\Delta \nu_Q^A = 1.3$ MHz and $\Delta \nu_Q^B = 3.7$ MHz. As we expect $\eta \lesssim 0.1$ the measured NQR frequencies will be indistinguishable from ν_Q given the large linewidths and overlapping lines. Now we have information on the distribution of the EFG magnitudes. This was used as input to Eq. (1) or (2) when extracting the EFG tilt distribution from the NMR line shapes. In addition to the line shape parameters for the *A* and *B* lines we find the integrated intensities. Corrected for spin echo delay, these yield the surprising result that 60% of the sites are *B* sites.

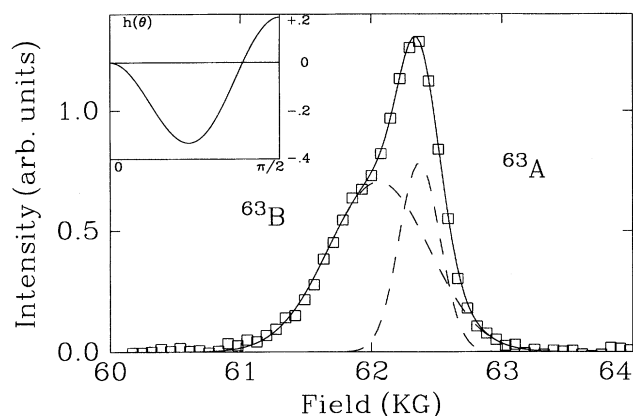


FIG. 4. NMR central transition line shape for $c \perp H_0$ taken at $T = 50$ K. The solid line is a fit to the data and the dashed lines are the A and B components of this fit. The inset shows $h(\theta)$ which governs the angle dependence of the second order quadrupolar component to the line shape.

We have studied the central transition line shape to learn about the orientation of the EFG's relative to the crystal c axis. This provides information about the local structural environment of the two types of copper sites. There will be a distribution of orientations of the EFG. Ideally we would like to obtain the functional dependence of this distribution on θ for each site. In practice we can obtain an average offset angle and a distribution width. As we will discuss here, the result is that on average the EFG at a B site is more tilted than at an A site. However we are unable to distinguish between two cases: (a) a narrow distribution with a peak at a nonzero tilt and (b) a uniform distribution of tilts out to a cutoff angle.

We have chosen the $c \perp H_0$ orientation to study the central transition line shape. At $\theta = 90^\circ$ the resonant frequency is shifted from the Larmor frequency by $3/16(\nu_Q^2/\nu_L)$. Three effects contribute to the linewidth: the ν_Q distribution, the θ distribution, and the ϕ distribution (the Knight shift width has been measured and found insignificant). As η is small, the contribution of the ϕ distribution is small and as the ν_Q distribution is known from the NQR spectra, the measured line shape can be used to extract some knowledge of the θ distribution. The line shape depends on θ through the function $h(\theta)$ displayed in the inset of Fig. 4. Spectra are collected for a series of angles near $\theta_0 = 90^\circ$. Here θ_0 is the angle between the crystal c axis and the applied field H_0 . We then follow two procedures to extract the desired information. The first and simplest involves assuming a convenient form for the EFG tilt distribution, fitting the measured line shapes and then extracting the EFG tilt distribution width $\Delta\theta$ from the angle dependence of the linewidths. The second procedure involves calculating the line shape directly using the NQR parameters as input. Various θ distributions are assumed and the resulting calculated line shapes compared with experiment.

Displayed in Fig. 4 is the central transition line shape for ^{63}Cu with $\theta_0 = 90^\circ$. The EFG tilt distribution is taken with respect to the c axis. The line shape is fit to two Gaussian components. The peak positions and FWHM are plotted as a

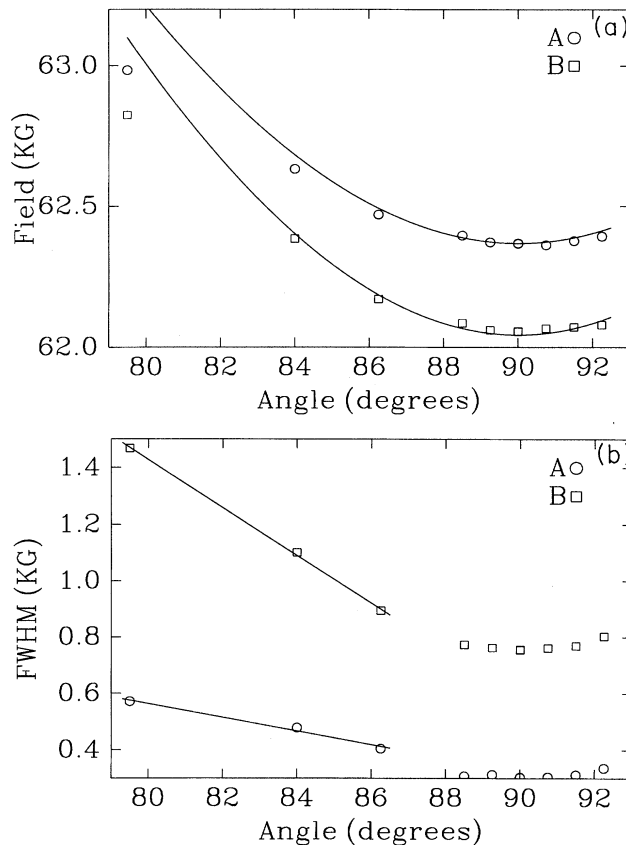


FIG. 5. (a) Central transition field and (b) FWHM vs angle for A (circles) and B (squares) resonances. The lines in (a) are the calculated position expected for the peak position. The lines in (b) depict the linear behavior expected for large deviations from 90° as described in the text.

function of θ_0 in Figs. 5(a) and 5(b), respectively. We now assume that the EFG principle axes are distributed uniformly about the crystal c axis out to a cutoff angle θ_c . For deviations of θ_0 about 90° which are $\geq \theta_c$ this model predicts that the mean square linewidth $\approx 15/8(\nu_Q^2/\nu_0)\theta_c|\pi/2 - \theta_0|$. Using the slopes from Fig. 5(b) we find that $\theta_c^A = 1.6^\circ$ and that $\theta_c^B = 4.6^\circ$. Thus we see that the EFG tilt distribution for the B sites is considerably larger than that for the A sites. This is consistent with the hypothesis that the B sites are associated with domains containing interstitial oxygen.

Generating line shapes using Eq. (1) for comparison with experiment leads to a similar conclusion for the EFG tilt distribution. We use the fitted ν_Q distribution obtained from the NQR spectrum as input with a chosen model for the EFG tilt distribution. Even though the EFG asymmetry parameter does not contribute much to the linewidth near $c \perp H_0$ it is nevertheless not zero. In order to get some idea of what η is we look at the satellite line shapes generated by this procedure. For $c \perp H_0$ about one-half of the satellite linewidth is due to the asymmetry parameter. We find that $\eta^A \approx 0.02$ and that $\eta^B \approx 0.07$. These values are used in Eq. (1) where we average over ϕ . We are now ready to generate line shapes for various models of the EFG tilt distribution.

Starting with the uniform EFG tilt distribution with cutoff

angle θ_c used above we find a good fit with $\theta_c^A = 2.0^\circ$ and $\theta_c^B = 4.3^\circ$. This is in reasonable agreement with the analysis of our simple model described above. Neutron scattering results indicate that all the apical oxygens may be tilted. A better tilt distribution may be a Gaussian peaked at an offset angle θ_{off} with a FWHM of $\Delta\theta$. A good fit is obtained with $\theta_{\text{off}}^A = 2.0^\circ$, $\theta_{\text{off}}^B = 3.0^\circ$, $\Delta\theta^A = 1.0^\circ$, and $\Delta\theta^B = 1.0^\circ$. These results are again consistent with our simple model. Given the number of parameters entering the line shape we cannot say which one of these, or other models we have tried, best fit the measured central transition line shape. Both methods demonstrate that B sites are characterized by a larger average tilt of the EFG.

We now compare our NMR results with the neutron diffraction results of Radaelli *et al.*³ They scattered neutrons from similarly prepared samples with $\delta = 0.08, 0.10,$ and 0.12 . As mentioned above they find that the excess oxygen occupies interstitial sites, confirming earlier work by Chaillout *et al.*¹¹ In addition they find it necessary to allow some of the apical oxygens to displace from their normal sites. The normal apical sites are not precisely located above the copper sites but tilted by about 4° . The apical oxygens neighboring the occupied interstitial sites are tilted further to about 15° . Considering what effect this has on the EFG tilt we should keep in mind that in the stoichiometric ($\delta = 0$) compound the octahedra order into a state with a tilt of about 4° about the orthorhombic (100) axis. In contrast, Radaelli *et al.* find that in the oxygen rich materials the tilt of the octahedra exhibit no long range order. However, a simple model of the EFG considering only the oxygen ions in a given octahedron indicates that a single interstitial oxygen neighbor will distort the octahedron such that the tilt of the EFG is about 7° .

Comparing the neutron scattering tilts with our EFG tilts yields qualitative agreement with the overall magnitudes being a bit larger in the former case. This is to be expected as the EFG results from a lattice sum which includes not just the nearest neighbors but further neighbors which are not affected as much by the presence of the interstitial. Thus the EFG tilt should be less than the tilt of the copper octahedron.

Both the larger distribution of tilts and the lower symmetry of the anomalous site can be straightforwardly understood as reflecting the proximity of an interstitial oxygen. The presence of the interstitial oxygen in the La-O layer forces away nearest neighbor apical oxygens. One can thus expect that the EFG at the corresponding copper sites will experience larger tips away from the c axis than will other sites. Furthermore this distortion will not be a rigid rotation of the octahedron but will significantly distort the octahedron, and we can expect to see a lowering symmetry such as is reflected by the much larger departure from axial symmetry observed for the B site, i.e., $\eta^B > \eta^A$. This observation provides strong evidence that the anomalous B sites are those nearest the interstitial oxygen.

It is now tempting to assign the B line exclusively to those copper nuclei whose apical oxygens are displaced by interstitial oxygens. As there are four nearest neighbor apical oxygens per interstitial site there should be $4\delta B$ sites, which for our crystal amounts to 40%. Recall that the actual NQR integrated intensity yields 60%. This suggests that the interstitial oxygens order. As a consequence of this ordering nearby apical oxygens will be displaced from their normal

positions to form some kind of a copper octahedra *tilt wave*. This may be accomplished through the vertical displacements of the planar oxygens of the octahedra which connect neighboring octahedra together. Thus more than just 4δ sites will be affected. Note that this is how the long range order in the octahedra tilt is established in the stoichiometric compound ($\delta = 0$). A line of planar oxygens along (100) lifts above the CuO_2 plane, thereby tilting a row of octahedra away from this line on either side.

Considering only the Cu NMR data we construct a plausible model for interstitial ordering based on the microscopic octahedral distortions. As there are four interstitial sites per planar oxygen in the unit cell and the average doping level is $\delta = 0.1$ every 5 unit cells will have one occupied interstitial site. Note that if every interstitial site was occupied $\delta = 2$. Hence start with a block of unit cells $5a \times 1b$ with only the left lowest interstitial site occupied. Now move diagonally up to the right by one unit cell. If this interstitial were to be occupied there would be a conflict between the two displaced apical oxygens moving closer to each other. Hence we occupy the interstitial site which is $1/2a$ to the left. The next occupied interstitial site will be as before which will be up to the right by two unit cells in both directions. This diagonal walk repeats to yield a supercell $5a \times 10b$. Moving up the c axis we displace the pattern by one unit cell to the right and then back one unit cell to the left for the next interstitial layer. This results in a total supercell of $5a \times 10b \times 1c$.

This ordering will result in the copper octahedra tilt pattern depicted in Fig. 6(a). The B domains contain all of the displaced apical oxygens whereas the A domains contain none. The size of these domains are consistent with the NQR integrated intensities. Folding in twinning we have a supercell of $10a \times 10b \times 1c$. This agrees with the supercell peaks observed by neutron scattering on a similar crystal³ in the a - b plane at least. Radaelli *et al.* see a supercell in their twinned crystal of $\text{La}_2\text{CuO}_{4.1}$ of $10a \times 10b \times 6c$.

To proceed further with the *tilt wave* we note that our previous NMR studies^{4,6} in $\text{La}_2\text{CuO}_{4+\delta}$ have revealed a distribution of tilts of the CuO_6 octahedra instead of the single, well-defined tilt expected in the orthorhombic phase. We found a simple tilt distribution: the probability of finding a given tilt θ is independent of θ for $\theta < \theta_{\text{max}}$, thus all tilts having $0 < \theta < \theta_{\text{max}}$ are equally likely. Stripe ordering has been observed¹⁴⁻¹⁶ in both Sr doped and O doped $\text{La}_{2-x}\text{Sr}_x\text{NiO}_4$. Additionally staging of the interstitial oxygen has been observed in $\text{La}_2\text{NiO}_{4+\delta}$.¹⁶ This leads us to consider such structures in the cuprate. A one-dimensional, sawtooth modulation of the octahedral tilt would provide a straightforward explanation for the observed uniform tilt distribution. The ^{139}La NMR measurements further reveal the existence of an upper cutoff in the tilts of the octahedra. We propose that in a given plane, the tilt of the oxygen octahedra is proportional to displacement r along the ordering wave vector thus forming a *tilt wave*.

Following our plausibility argument above we assign this wave vector to be diagonal with respect to the orthorhombic cell. In order for the *tilt wave* to be consistent with the ^{139}La NMR data we suggest that when the tilt of the octahedra reach a critical value θ_{max} , it abruptly changes sign, then continues to linearly increase: $\theta_{\text{tilt}} = (2\theta_{\text{max}}/\lambda)[\text{modulo } (r, \lambda) - 1/2]$ where λ is the wavelength of the modulation

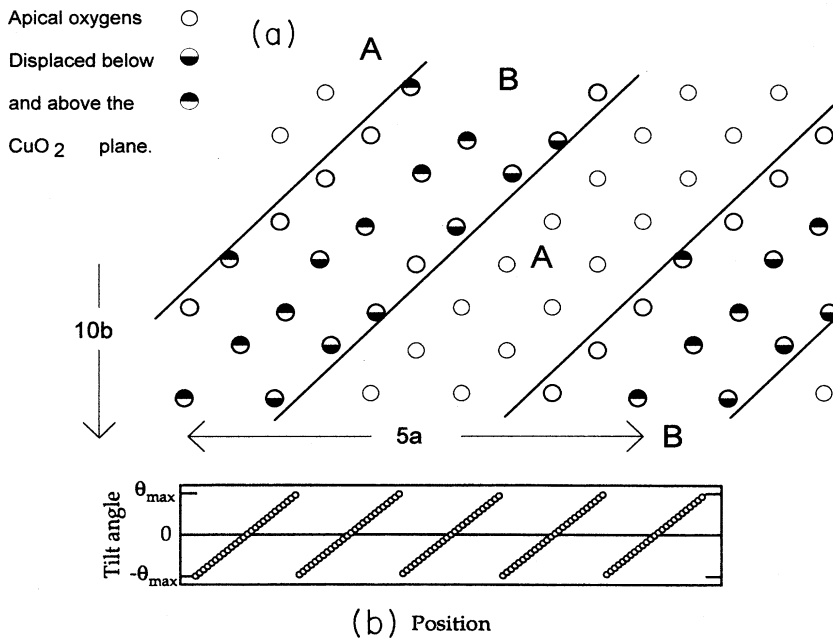


FIG. 6. Interstitial ordering and tilt wave. (a) Striped domains in the CuO_2 plane. (b) Proposed sawtooth variation of the octahedral tilt with displacement along the wavevector for the tilt modulation is shown. The large openings in the La-O layer produced by the abrupt shift in tilt from θ_{\max} to $-\theta_{\max}$ would provide a favorable site for the interstitial oxygen.

wave, taken to be $5\sqrt{2}a$ (a =lattice constant along the orthorhombic a axis) in accordance with the neutron diffraction results.³ [Here, we take the sign of $\text{modulo}(x,y)$ to have the sign of x .] We show this tilt pattern in Fig. 6(b). This tilt modulation is closely related with ordering of the oxygen because at the point where the tilt changes sign, the large difference in tilt angle will leave a large opening in the La_2O_2 layer between neighboring apical oxygens which can accommodate extra interstitial oxygen. Given that Radaelli *et al.* have observed a supercell with size perpendicular to the layers of $6c$ it may be that staging occurs with excess oxygen occupying less than every possible layer.

The copper NMR results demonstrate that the anomalous copper sites are adjacent to the interstitial oxygen. Thus the anomalous copper B sites would inhabit striped domains centered on the stripe-ordered interstitial oxygen. It is clear, however, that the proximity to interstitial oxygen alone cannot be responsible for distinguishing the anomalous copper site in NQR spectra. The nearly identical values for the NQR frequency in Sr and O doped lanthanum cuprate make clear that the second site is distinguished by the presence of doped holes independently of the means of doping. This point has been verified by *ab initio* cluster calculations by Martin¹⁷ which show that the shift due to the two different dopants alone differs by a factor of 10 (Sr shifts the NQR resonance by 0.5 MHz while O shifts it by almost 4.5 MHz). However, Martin finds that the presence of a hole localized on a neighboring Cu site produces essentially the exact shift, 2.5 MHz, observed in experiment between the B and A sites (see Fig. 3). In addition to the close agreement with the measured frequency, this mechanism provides an attractive explanation for the anomalous site in that it depends only on the presence of doped holes and so can simultaneously explain the spectra obtained in Sr and O doped materials. Since there are four nearest neighbors to a given copper site occupied by a localized hole, the intensity of the anomalous B line predicts that

roughly half of the doped holes are localized in our sample ($\delta \approx 0.10$) of $\text{La}_2\text{CuO}_{4+\delta}$ (the remainder of the doped holes are itinerant). The association of these localized holes with the ordered interstitial oxygen leads to the possibility of stripes of localized holes in the CuO_2 planes. It is important to note that other cuprates exhibit similar stripe ordering of localized holes. Using extended x-ray-absorption fine structure (EXAFS) Bianconi *et al.*¹⁸ have observed polaronic stripes in the $\text{Bi}(2212)$ material in which polarons order into stripes.

Taking the localized holes to reside in the B domains how do the itinerant carriers behave? The Knight shift K and spin-lattice relaxation rate T_1^{-1} provide some indication of the local electronic environment. We find that $K_A = K_B = 0.50\%$ at $T = 50$ K. As the Knight shift in the normal state consists of the orbital K_{orb} and spin K_s components we cannot say with certainty that K_s in the two domains are equal. We also find $T_1 = 0.30$ msec for both A and B sites. The similarity in electronic properties at the two sites suggests that the itinerant hole densities in the two domains are not that different. Thus the behavior of the itinerant holes averages over the A and B domains.

Localized holes residing in the B striped domains could have important ramifications for the apparent inconsistency of oxygen NMR and inelastic neutron scattering (INS) results in strontium doped lanthanum cuprate. NMR finds commensurate antiferromagnetic spin fluctuations (AFSF) whereas INS finds the spin fluctuations to be incommensurate.^{19,20} INS is a probe of average structure whereas NMR is a very local probe. Locally commensurate AFSF could then appear incommensurate if there is an ordered structure of objects which can alter the phase of the AFSF. We have presented results which provide evidence for localized holes in the CuO_2 planes of O doped lanthanum cuprate. These would certainly alter the antiferromagnetic interactions and thus could break the phase memory of the

commensurate spin fluctuations. Furthermore we have argued for stripe ordering of the phase-breaking domain walls in O doped materials which could lead to the appearance of a well-defined incommensurate scattering peak in INS. However, to understand the result in $\text{La}_{2-x}\text{Sr}_x\text{CuO}_4$ will require the demonstration that the localized holes order in this compound as well, and with an appropriate wavelength to explain the observed neutron scattering peak.

We have considered a variety of results from magnetic resonance and neutron scattering experiments together with the well-established observation of charge ordering in O doped lanthanum nickelate into stripes. We have argued that in O doped lanthanum cuprate the interstitial oxygen orders into stripes. The lattice participates in this ordering through a long wavelength modulation of the octahedral tilts. When the tilt reaches a maximum value it shifts to a tilt equal in magnitude but in the opposite direction. We have shown that the anomalous copper B site in the CuO_2 plane neighbors the interstitial oxygens. Calculations indicate that the anomalous copper site is one which also neighbors a localized hole. This

relationship of stripe-ordered interstitial oxygen to localized hole leads to a picture of localized or pinned holes forming striped domains in the CuO_2 planes. These ordered localized holes may be responsible for the apparent discrepancy between inelastic neutron scattering and NMR results regarding the spin-fluctuation spectrum.

ACKNOWLEDGMENTS

We gratefully acknowledge stimulating discussions with Richard L. Martin who has shared the results of his calculations prior to publication. We also acknowledge stimulating discussions with D. Pines, S. Trugman, and A. J. Millis. This work at Los Alamos was performed under the auspices of the U.S. Department of Energy. Ames Laboratory is operated for the U.S. Department of Energy under Contract No. 2-405-Eng-82. The work at Ames was supported by the Director for Energy Research, Office of Basic Energy Sciences. B.W.S. acknowledges support from the Natural Sciences and Engineering Research Council of Canada.

*Permanent address: Department of Physics, University of Toronto, Toronto, Canada M5S 1A7.

¹See *Phase Separation in Cuprate Superconductors*, edited by E. Sigmund and K.A. Müller (Springer-Verlag, Berlin, 1994).

²S.A. Kivelson and V.J. Emery, in *Strongly Correlated Electronic Materials*, edited by K.S. Bedell, Z. Wang, D.E. Meltzer, A.V. Balatsky, and E. Abrahams (Addison-Wesley, Reading, MA, 1994), p. 619; V.J. Emery and S.A. Kivelson, *Physica C* **209**, 597 (1993); J.H. Cho, F.C. Chou, and D.C. Johnston, *Phys. Rev. Lett.* **70**, 222 (1993); F.C. Chou, F. Borsa, J.H. Cho, D.C. Johnston, A. Lascialfari, D.R. Torgeson, and J. Ziolo, *ibid.* **71**, 2323 (1993).

³P.G. Radaelli, J.D. Jorgensen, A.J. Schultz, B.A. Hunter, J.L. Wagner, F.C. Chou, and D.C. Johnston, *Phys. Rev. B* **48**, 499 (1993).

⁴P.C. Hammel, A.P. Reyes, S-W. Cheong, Z. Fisk, and J.E. Schirber, *Phys. Rev. Lett.* **71**, 440 (1993).

⁵K. Ueda, T. Sugata, Y. Kohori, T. Kohara, Y. Oda, M. Yamada, S. Kashiwai, and M. Motoyama, *Solid State Commun.* **73**, 49 (1990); T. Kohara, K. Ueda, Y. Kohori, and Y. Oda, *Physica C* **185-189**, 1189 (1991); T. Tsuda, T. Ohno, and H. Yasuoka, *J. Phys. Soc. Jpn.* **61**, 2109 (1991); Y.-Q. Song, M.A. Kennard, M. Lee, K.R. Poeppelmeier, and W.P. Halperin, *Phys. Rev. B* **44**, 7159 (1991); S. Ohsugi *et al.*, *J. Phys. Soc. Jpn.* **60**, 2351 (1991); K. Kumagai *et al.*, *Z. Naturforsch Teil A* **45**, 433 (1990).

⁶P.C. Hammel, A.P. Reyes, E.T. Ahrens, D.E. MacLaughlin, J.D. Thompson, Z. Fisk, P.C. Canfield, S-W. Cheong, and J. E. Schirber, *Physica B* **199-200**, 235 (1994).

⁷P.G. Radaelli, J.D. Jorgensen, R. Kleb, B.A. Hunter, F.C. Chou, and D.C. Johnston, *Phys. Rev. B* **49**, 6239 (1994).

⁸Bernd Büchner, Ph.D. thesis, II. Physikalisches Institut, University of Köln, 1993; B. Büchner, M. Breuer, A. Freimuth, and A.P. Kampf, *Phys. Rev. Lett.* **73**, 1841 (1994).

⁹P.C. Hammel, A.P. Reyes, Z. Fisk, M. Takigawa, J.D. Thompson,

R.H. Heffner, S-W. Cheong, and J.E. Schirber, *Phys. Rev. B* **42**, 6781 (1990).

¹⁰The oxygen content was originally reported to be 4.032 (Refs. 4 and 6) based on neutron diffraction measurement in a similarly prepared crystal (see Ref. 11). The oxygen content of our crystal was not measured. The overall oxygen content we report here (4.04) is within the error in the earlier measurement and has been modified to achieve consistency with the data of Radaelli (Ref. 7). Radaelli *et al.* report an uncertainty of 0.01 in their oxygen contents. Note also that Radaelli's data were taken in powders whereas the NMR sample was a crystal. It is possible that because of differing strains in powders and crystals, these transitions may be different in the two cases.

¹¹C. Chailout, S-W. Cheong, Z. Fisk, M.S. Lehmann, M. Marezio, B. Morosin, and J.E. Schirber, *Physica C* **158**, 183 (1989); **158**, 183 (1989); C. Chailout, J. Chenavas, S-W. Cheong, Z. Fisk, M. Marezio, B. Morosin, and J.E. Schirber, *ibid.* **C 170**, 87 (1990).

¹²T. Imai, C.P. Slichter, K. Yoshimura, and K. Kosuge, *Phys. Rev. Lett.* **70**, 1002 (1993).

¹³F.C. Chou, D.C. Johnston, S-W. Cheong, and P.C. Canfield, *Physica C* **216**, 66 (1993).

¹⁴Z. Hiroi, T. Obato, M. Takano, Y. Bando, Y. Takeda, and O. Yamamoto, *Phys. Rev. B* **41**, 11 665 (1990).

¹⁵C.H. Chen, S-W. Cheong, and A.S. Cooper, *Phys. Rev. Lett.* **71**, 2461 (1993).

¹⁶J.M. Tranquada, D.J. Buttrey, V. Sachan, and J.E. Lorenzo, *Phys. Rev. Lett.* **73**, 1003 (1994).

¹⁷R. Martin (unpublished).

¹⁸A. Bianconi and M. Missori, *Phase Separation in Cuprate Superconductors* (Ref. 1), p. 272, and references therein.

¹⁹S-W. Cheong *et al.*, *Phys. Rev. Lett.* **67**, 1791 (1991); T.E. Mason, G. Aeppli, and H.A. Mook, *ibid.* **68**, 1414 (1992).

²⁰V. Barzykin, D. Pines, and D. Thelen, *Phys. Rev. B* **50**, 16 052 (1994).